Contents lists available at ScienceDirect

Journal of the Mechanical Behavior of Biomedical Materials

journal homepage: www.elsevier.com/locate/jmbbm

Indirect 3D bioprinting and characterization of alginate scaffolds for potential nerve tissue engineering applications

Saman Naghieh[a,*], M.D. Sarker[a], Emily Abelseth[b], Xiongbiao Chen[a,c,*]

[a] Division of Biomedical Engineering, College of Engineering, University of Saskatchewan, Saskatoon, SK, Canada
[b] Department of Biomedical Engineering, Faculty of Engineering, University of Victoria, Victoria, BC, Canada
[c] Department of Mechanical Engineering, College of Engineering, University of Saskatchewan, Saskatoon, SK, Canada

ARTICLE INFO

Keywords:
3D bioprinting
Indirect bioprinting
Nerve tissue engineering
Mechanical properties
Cell viability
Alginate

ABSTRACT

Low-concentration hydrogels have favorable properties for many cell functions in tissue engineering but are considerably limited from a scaffold fabrication point of view due to poor three-dimensional (3D) printability. Here, we developed an indirect-bioprinting process for alginate scaffolds and characterized the potential of these scaffolds for nerve tissue engineering applications. The indirect-bioprinting process involves (1) printing a sacrificial framework from gelatin, (2) impregnating the framework with low-concentration alginate, and (3) removing the gelatin framework by an incubation process, thus forming low-concentration alginate scaffolds. The scaffolds were characterized by compression testing, swelling, degradation, and morphological and biological assessment of incorporated or seeded Schwann cells. For comparison, varying concentrations of alginate scaffolds (from 0.5% to 3%) were fabricated and sterilized using either ultraviolet light or ethanol. Results indicated that scaffolds can be fabricated using the indirect-bioprinting process, wherein the scaffold properties are affected by the concentration of alginate and sterilization technique used. These factors provide effective means of regulating the properties of scaffolds fabricated using the indirect-bioprinting process. Cell-incorporated scaffolds demonstrated better cell viability than bulk gels. In addition, scaffolds showed better cell functionality when fabricated with a lower concentration of alginate compared to a higher concentration. The indirect-bioprinting process that we implemented could be extended to other types of low-concentration hydrogels to address the tradeoffs between printability and properties for favorable cell functions.

Indirect 3D bioprinting and characterization of alginate scaffolds for potential nerve tissue engineering applications

Saman Naghieh, M.D. Sarker, Emily Abelseth, Xiongbiao Chen

PII: S1751-6161(18)30218-2
DOI: https://doi.org/10.1016/j.jmbbm.2019.02.014
Reference: JMBBM3162

To appear in: *Journal of the Mechanical Behavior of Biomedical Materials*

Received date: 23 February 2018
Revised date: 5 November 2018
Accepted date: 13 February 2019

Cite this article as: Saman Naghieh, M.D. Sarker, Emily Abelseth and Xiongbiao Chen, Indirect 3D bioprinting and characterization of alginate scaffolds for potential nerve tissue engineering applications, *Journal of the Mechanical Behavior of Biomedical Materials,* https://doi.org/10.1016/j.jmbbm.2019.02.014

Indirect 3D bioprinting and characterization of alginate scaffolds for potential nerve tissue engineering applications

Saman Naghieh [1*], MD Sarker [1], Emily Abelseth [2], Xiongbiao Chen [1,3*]

[1]Division of Biomedical Engineering, College of Engineering, University of Saskatchewan, Saskatoon, SK, Canada

[2]Department of Biomedical Engineering, Faculty of Engineering, University of Victoria, Victoria, BC, Canada

[3]Department of Mechanical Engineering, College of Engineering, University of Saskatchewan, Saskatoon, SK, Canada

PII: S1751-6161(18)30218-2
DOI: https://doi.org/10.1016/j.jmbbm.2019.02.014
Reference: JMBBM3162

* Corresponding authors: Division of Biomedical Engineering, College of Engineering, University of Saskatchewan, Saskatoon, SK, Canada.

Email address: san908@mail.usask.ca (Saman Naghieh) and xbc719@mail.usask.ca (Xiongbiao Chen).

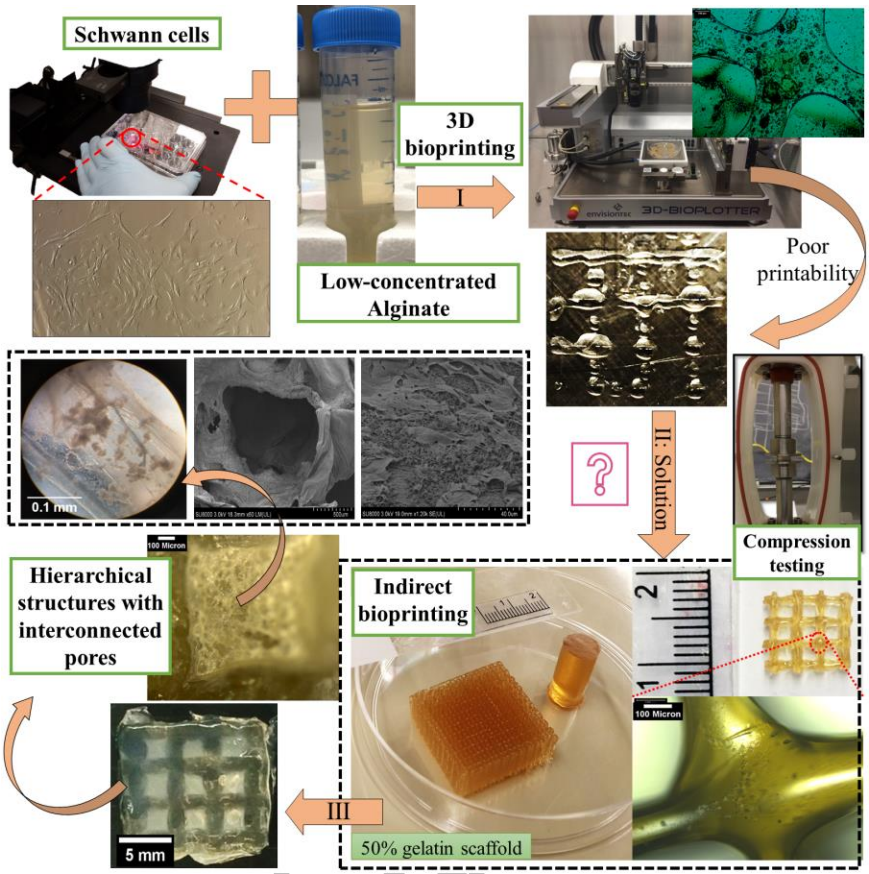

Abstract

Low-concentration hydrogels have favorable properties for many cell functions in tissue engineering but are considerably limited from a scaffold fabrication point of view due to poor three-dimensional (3D) printability. Here, we developed an indirect-bioprinting process for alginate scaffolds and characterized the potential of these scaffolds for nerve tissue engineering applications. The indirect-bioprinting process involves (1) printing a sacrificial framework from gelatin, (2) impregnating the framework with low-concentration alginate, and (3) removing the gelatin framework by an incubation process, thus forming low-concentration alginate scaffolds. The scaffolds were characterized by compression testing, swelling, degradation, and morphological and biological assessment of incorporated or seeded Schwann cells. For comparison, varying concentrations of alginate scaffolds (from 0.5 to 3%) were fabricated and sterilized using either ultraviolet light or ethanol. Results indicated that scaffolds can be fabricated using the indirect-bioprinting process, wherein the scaffold properties are affected by

the concentration of alginate and sterilization technique used. These factors provide effective means of regulating the properties of scaffolds fabricated using the indirect-bioprinting process. Cell-incorporated scaffolds demonstrated better cell viability than bulk gels. In addition, scaffolds showed better cell functionality when fabricated with a lower concentration of alginate compared to a higher concentration. The indirect-bioprinting process that we implemented could be extended to other types of low-concentration hydrogels to address the tradeoffs between printability and properties for favorable cell functions.

Keywords: 3D bioprinting; indirect bioprinting; nerve tissue engineering; mechanical properties; cell viability; alginate

1. Introduction

Recent progress in tissue engineering has placed the possibility of meeting the growing worldwide demand for tissue and organ replacements within reach in the near future. To this end, extrusion-based bioprinting has played an important role in fabricating complex structures layer-by-layer to mimic native tissues (Naghieh et al., 2018b; Naghieh and Chen, 2019; Vijayavenkataraman et al., 2018). Hydrogels have often been used in the extrusion-based technique as a bioink to incorporate large cell populations, growth factors, proteins, and peptides (Tan et al., 2016). Notably, properties of a hydrogel bioink depend on its hydrogel concentration and affect cell viability (Matyash et al., 2012), printability (Bertassoni et al., 2014; He et al., 2016), and mechanical strength of the printed scaffolds (Skardal et al., 2015). At low concentrations, hydrogels are difficult, and at times even impossible, to print three-dimensional (3D) constructs. In contrast, hydrogels at relatively high concentrations can reduce cell viability due to the increased mechanical strength of hydrogels (Ning et al., 2018) and higher induced forces that cells experience during the fabrication process (Li et al., 2009). The hydrogel concentration can also influence mechanical properties (LeRoux et al., 1999). Further investigation into these influences is urged (He et al., 2016).

By means of the extrusion-based technique, scaffolds made from hydrogels have been explored for nerve tissue engineering (England et al., 2017; Ning et al., 2018; Potjewyd et al., 2018). In nerve tissue engineering, considerable evidence supports the use of low-concentration hydrogels due to their favorable effects on cell responses or functions (Matyash et al., 2012). It has also been reported that low-concentration alginate (0.2 and 1% (w/v) is able to provide a

better environment for neurite growth and cell viability (Cao et al., 2012; Matyash et al., 2012). While low-concentration alginate can support nerve tissue regeneration, poor printability makes it an undesirable material for printing scaffolds (Matyash et al., 2012; Ning et al., 2016). Hydrogels at higher concentrations have been used to enhance the printability and structural fidelity but at the cost of reduced in-growth of new tissue (Augst et al., 2006). Therefore, approaches that allow for addressing this issue are greatly needed. Among these approaches, indirect printing has been evolved promising to tackle the poor printability of low concentration hydrogels (Houben et al., 2017; Tan et al., 2010; Yeong et al., 2006).

Indirect bioprinting involves the creation of a sacrificial framework, which is used temporarily to support the formation of a scaffold made of a polymer (Tamjid and Simchi, 2015). Using indirect bioprinting, different materials, including bioactive materials and cells, can be strategically incorporated in a scaffold. Furthermore, indirect bioprinting allows for control over both the external and internal structure, thus creating scaffolds with advanced architecture (Yeong et al., 2006). As such, indirect bioprinting offers a great degree of versatility with respect to materials and structures, making it an attractive technique for the creation of complex hydrogel scaffolds. Notably, indirect 3D bioprinting of hydrogel scaffolds for nerve tissue regeneration has not been explored. Specifically, the mechanical and biological properties of hydrogel scaffolds fabricated by the indirect approach remain unclear, raising the need to discover their applications in nerve tissue regeneration.

As inspired, we developed an indirect bioprinting process for fabricating alginate scaffolds so as to address the issue of poor printability of low-concentration alginate. Our stepwise study included i) fabricating 0.5, 1.5, and 3% alginate scaffolds via the indirect bioprinting process where 50% gelatin is used as the sacrificial framework; ii) investigating the effects of UV and ethanol sterilization techniques on the mechanical properties of the indirectly-bioprinted scaffolds; iii) examining the degradation and swelling of the indirectly-bioprinted scaffolds; and iv) assessing the biological properties of the indirectly-bioprinted scaffolds. In addition, bulk gels and directly-bioplotted scaffolds were assessed and compared in terms of the viability of incorporated Schwann cells using a live/dead assay. The novelty of this work lies in the development of a method to create scaffolds from low-concentration alginate to circumvent its poor printability occurring in the direct bioprinting process. To the best of our knowledge, this

is the first report of mechanically-stable scaffolds fabricated by an indirect printing technique and made of low-concentration alginate, with potential for nerve tissue engineering.

2. Materials and Methods

2.1.Materials and equipment

Gelatin (from bovine skin), medium viscosity sodium alginate (sodium salt from brown algae, medium viscosity), calcium chloride ($CaCl_2$), Dulbecco's modified Eagle's medium (DMEM), fetal bovine serum (FBS), trypsin, ethylene-diaminetetraacetic acid (EDTA), and fluorescent dyes (propidium iodide (PI), calcein, Hoechst 33342) were all obtained from Sigma Aldrich (St. Louis, MO). Phosphate buffered saline (PBS; 0.0067 M) was obtained from HyClone (Logan, Utah). Primary rat Schwann cells (PRSCs) were supplied by Saskatoon City Hospital. A Sartorius scale (model 225d; Shanghai, China) was used for weighing samples. A 0.22-μm bottle-top filter (Thermo Scientific, Ann Arbor, MI, USA) was used to filter alginate solutions. A freeze-dryer (FreeZone, Labconco, USA) was used to freeze-dry samples. Sterile circular coverslips (Thermo Scientific™) and 12/24-well tissue culture plates (Thermo Fisher Scientific, MA, USA) were used for experiments.

2.2. Directly bioprinting of scaffolds and preparation of cell-incorporated bulk gels

2.2.1. Direct bioprinting of scaffolds

3D scaffolds were directly printed on a 3D bioplotter (EnvisionTEC, Germany). For this, 12-well plates were coated with polyethyleneimine (PEI) for the purpose of enhancing the attachment of first printing layer to the plate during the printing process (Rajaram et al., 2015) and then the coated plates were placed in an incubator over a day for the subsequent use in scaffold printing. Three hydrogels, comprised of 0.5, 1.5, and 3% alginate, representing low to reasonably high concentrations, were chosen to investigate the mechanical and biological performance of scaffolds fabricated by using a direct printing technique. For all groups, 300 μL of sterile alginate were mixed with 20 μL of cell media (for cell preparation procedure refer to §2.2.2). The mixture was transferred to a 200-μm needle and three samples of each concentration were printed in a lattice pattern into PEI-coated wells (Figure 1). Printing parameters were chosen based on a printability study, which aimed to identify the appropriate temperature, pressure, and linear speed for each alginate concentration (results not shown). The print

temperature for the 3% alginate was set at 20 °C, and the pressure and linear speed of the head were 0.3 bar and 14 mm/s, respectively. The print temperature for the 1.5% alginate was also 20 °C and the pressure and linear speed were set to 0.1 bar and 26 mm/s, respectively. The inter-strand distance was 3.5 mm for all groups. After printing one layer, 1 mL of $CaCl_2$ was added, then removed after 2 min and replaced with 1 mL of DMEM. The 0.5% alginate solution had poor printability (inconsistent strands and beading) and was not printable with a 100-µm needle (Figure 1c); using a 200-µm needle resulted in a bulk gel with no visible lattice structure. Therefore, instead of direct bioprinting of 0.5% alginate, bulk gel was used for further studies. To this end, 100 µL of the mixture (0.5% alginate and cells) was transferred into three separate wells. Then 1 mL of $CaCl_2$ was immediately added to each well, removed, and replaced with 1 mL of DMEM. The plates were incubated at 37 °C and 5% CO_2.

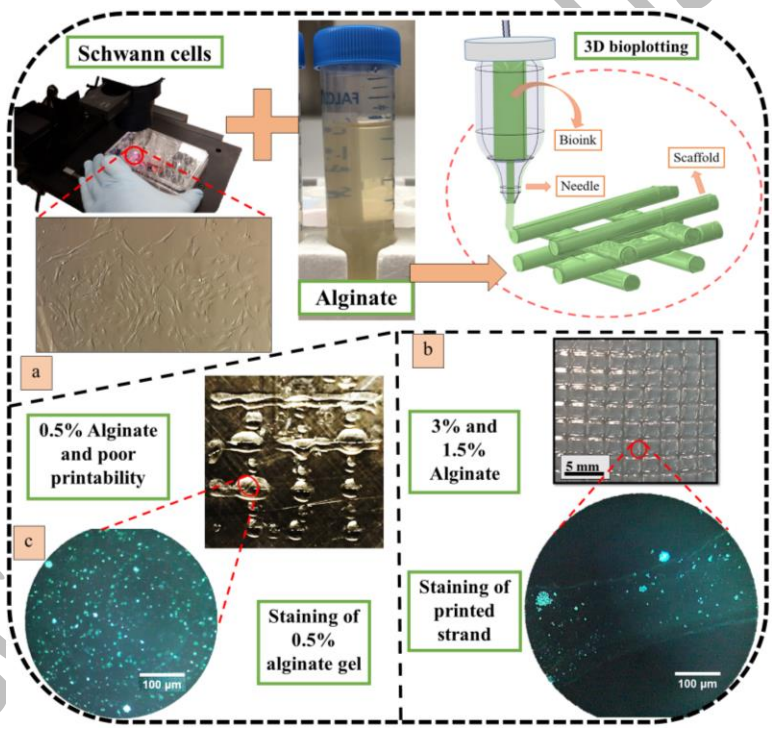

Figure 1. 3D bioplotting of alginate hydrogels: a) cultivated Schwann cells mixed with alginate hydrogel and then bioplotted, b) cell-incorporated alginate scaffold and staining result showing one strand, and c) poor printability of 0.5% alginate printed with a 100-µm needle and staining result of cell-incorporated gel.

2.2.2. Preparation of alginate solutions with cells

A culture dish with PRSCs was examined under a microscope to assess the confluency of cells for that 85-100% is required for cell passing; and for all cell-viability studies, the passage number of cells were maintained between 6 and 14. The culture medium was completely aspirated, then 5 mL of 10 mM sterile PBS was added along the sides of the plate, gently swirled, then completely aspirated. One mL of sterile trypsin + EDTA was added, and the plate was gently swirled so the mixture coated the entire surface of the plate. The trypsin + EDTA was aspirated, and the plate was incubated for 5 min at 37°C and 5% CO_2. Six mL of DMEM + 10% FBS were added and gently re-pipetted to create an even suspension. The entire contents of the culture dish were transferred to a 14-mL Falcon tube and centrifuged at 800 rpm for 5 min. After centrifuging, 300 μL of the solution were kept in the Falcon tube and the cell pellet redistributed in the solution. Cell density was 500,000 cells per 300 μL of solution. Then 80 μL of this solution were added to each alginate sample (0.5, 1.5, and 3.0%), and then mixed with a multi-rotator for 5 min.

2.2.3. Preparation of cell-incorporated Bulk Gels

A 0.22-μm bottle-top filter was used to filter 0.5% (w/v) medium viscosity sodium alginate solution, which was kept in a freezer at −80 °C for 24 h and then freeze-dried for 48 h, while maintaining a sterile environment. The freeze-dried alginate was re-dissolved in sterile calcium-free DMEM to prepare 0.5, 1.5, and 3% (w/v) alginate precursors. PRSCs were cultured and trypsinized as per §2.2.2. Alginate precursors were thoroughly mixed with the cells at a density of 5×10^5cells/mL to obtain a homogeneous cell distribution in the hydrogel. The mixture of alginate/cell suspension (100 μL) was poured onto sterile circle coverslips coated with 0.1% w/v PEI solution, and then 1 mL $CaCl_2$ (50 mM) solution was layered over the dispensed alginate solution to facilitate crosslinking for 6 min in a 24-well tissue culture plate.

2.3. Indirect bioprinting of alginate scaffolds

A 50% (w/v) gelatin solution was prepared by dissolving 20 g of gelatin in 40 mL of distilled water using a magnetic stir plate heated to 50 °C. The gelatin framework was designed using Magics CAD software (Materialise, Belgium), and then printed using a 3D bioplotter (EnvisionTEC, Germany), as shown in Figure 2. Strands were printed and layered on top of one another to form a 25 mm × 25 mm × 2.50 mm square lattice structure with a pore size of 2.5 mm.

A print pressure of 0.8 bar, temperature of 50 °C, speed of 16 mm/s, and a 24-gauge printing needle were used for printing; and structures were printed with 20 layers.

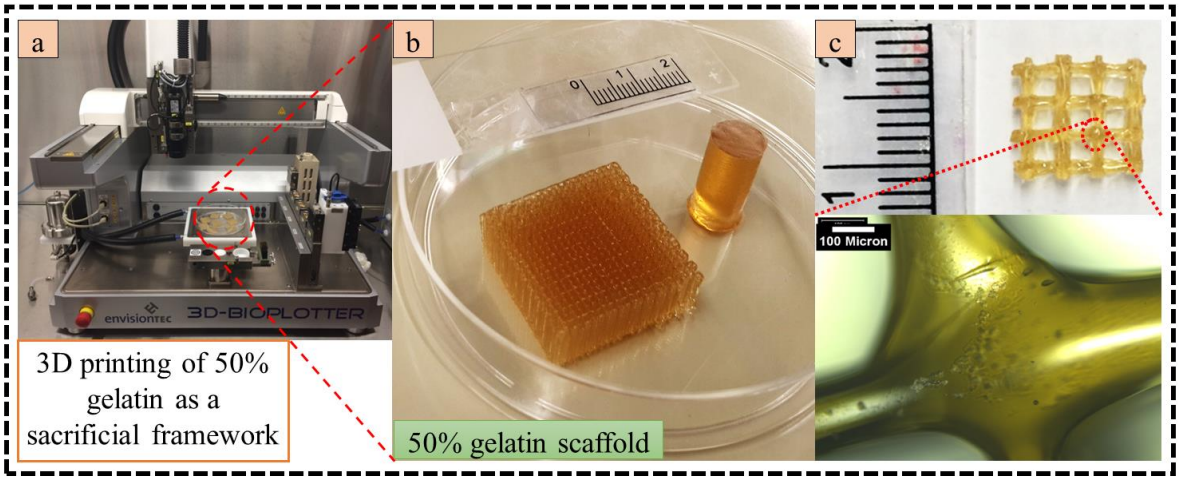

Figure 2. Indirect biofabrication: a) 3D bioplotter used for the fabrication of gelatin scaffolds, b) gelatin scaffold and bulk gel samples, and c) gelatin scaffold used for indirect biofabrication and a close-up view of this sacrificial framework.

The 0.5, 1.5, and 3.0% alginate solutions were prepared by dissolving 0.2, 0.6, or 1.2 g of alginate, respectively, into 40 mL of distilled water using a multi-rotator. A 50 mM $CaCl_2$ solution was prepared by mixing 2.2 g of $CaCl_2$ with 300 mL of distilled water. Gelatin frameworks were cut into smaller samples of approximately 8 mm × 8 mm × 2.5 mm and then placed in separate dishes. Alginate solution was added or impregnated to each of the gelatin frameworks and then 0.1 mL of 50 mM $CaCl_2$ added on top of the frameworks. The frameworks were then flipped and impregnated with more alginate. Excess alginate and bubbles in the pores were removed using a pipette, and 50 mM $CaCl_2$ was poured into the dishes. Dishes were refrigerated for 18 h, then placed in an incubator at 37 °C and 5.0% CO_2 for 48 h in order to melt and remove gelatin. Scanning electron microscopy (SEM) was used to investigate the morphology of the indirectly-printed scaffolds. SEM images were captured using a Hitachi microscope on gold-coated samples. Images were taken at each stage of the indirect-fabricated scaffold preparation to determine pore size and strand thickness and analyzed using ImageJ® software.

2.4. Sterilization of scaffolds by ethanol disinfection or UV irradiation

Ethanol disinfection was carried out as per the previous study (Stoppel et al., 2014). Three samples from each group of scaffolds were placed in separate dishes, and then 250 mL of 70% ethanol was pipetted into each dish. The samples were exposed for 20 min and then the ethanol was removed and replaced with 250 mL of distilled water. The samples were soaked in distilled water for 10 min before mechanical testing. UV sterilization involved placing samples in separate dishes underneath a 254 nm UV light source for 20 min, with aluminum foil used to enclose the area. Other sterilization techniques such as lyophilization, gamma-irradiation, and ethylene oxide treatment were not explored as they have been shown to negatively affect the alginate structure (Stoppel et al., 2014). Disinfection via ethanol or UV light was chosen to be investigated as these techniques have not been investigated in many studies.

For post-seeding of indirect-fabricated scaffolds, scaffolds of each concentration group were sterilized by soaking in 70% ethanol for 20 min, then transferred to sterile Falcon tubes, and freeze-dried for 48 h. Freeze-dried samples were placed in PEI-coated wells of a 12-well plate, then covered with 10 µL of cell mixture and 2 mL of DMEM. After 2 min, the DMEM was removed and an additional 5 µL of cell mixture was added along with 1 mL of DMEM. Scaffolds were kept in an incubator at 37 °C and 5% CO_2.

2.5. Mechanical tests

The mechanical properties of the scaffolds were tested by uniaxial unconfined compression on a BioDynamic 5010 testing machine (Bose, USA). Tests were repeated three times for each group of scaffolds. In each test, the geometrical features of scaffolds were measured and characterized by taking pictures of scaffolds and analyzing them using ImageJ software. The scaffolds were then placed between the two smooth plates of the testing machine and subjected to compression at a rate of 0.017 mm/s. A stress-strain curve was generated for each group of scaffolds, and the slope of the linear portion of the curve was evaluated to calculate the elastic modulus.

2.6. Assessment of the swelling and degradation rates

Swelling correlates with a hydrogel's ability to retain water and is an important property to understand to prevent adverse effects on the surrounding tissue when a scaffold is implanted *in vivo*. The rate of degradation is an important property to consider when creating a biomimetic scaffold as well (Sun and Tan, 2013). Samples made of varying concentrations of alginate

scaffolds (from 0.5 to 3%) were removed from the crosslinker solution and placed separately in pre-weighed dishes. Excess liquid was removed with a Kimwipe tissue and the weights of the dishes were recorded. In the next step, 2 mL of PBS were added to each dish, which were then incubated at 37 °C and 5% CO_2. At various time points (1, 2, 3, 4, 6, and 12 h, 1 d and 7 d), the dishes were removed from the incubator, the PBS was removed, the dishes were reweighed. Percent swelling was calculated as

$$\%\, Swelling = \frac{w_t - w_0}{w_0} \times 100,$$

where w_0 is the initial weight of the sample and w_t is the weight measured at one the above time points.

To study the degradation rate, 10 samples from each group were placed in pre-weighed Falcon tubes and then stored in the freezer at −40 °C for 4 h. Samples were then freeze-dried and weighed to determine their initial mass. Samples were then soaked in 1 mL of 70% ethanol for 20 min, the ethanol removed, and 2 mL of PBS added to each Falcon tube. The samples were then placed in an incubator at 37 °C and 5% CO_2 for 1, 3, 6, 24, or 48 h. At these time points, the PBS solution was removed, then the Falcon tubes placed in the freezer, freeze-dried, and reweighed. Degradation rate was calculated as

$$\%\, Degradation = \frac{w_{FD0} - w_{FDt}}{w_{FD0}} \times 100,$$

where w_{FD0} is the initial weight of the freeze-dried scaffold and w_{FDt} is the weight of the freeze-dried scaffold at one the above time points (1, 2, 3, 4, 6, and 12 h, 1 d and 7 d).

2.7. Cell viability and morphological assessment

Fluorescent microscope imaging of the bulk gels took place on days 1, 3, and 8 using a Zeiss Germany microscope (Axiovert 100) and X-cite® EXFO (series 120). Samples were stained with 5 mg/mL Hoechst and 50 mg/mL PI/Calcein dye. Imaging of the cell-incorporated scaffolds occurred on days 1, 4, and 8. Samples were stained with 5 mg/mL Hoechst and 1 mg/mL calcein, with 2 μL of each dye added to the samples and mixed with a pipette. Samples were then incubated for 1 h. DMEM was removed, samples were washed with PBS, 1 mL of fresh DMEM was added, and then the samples were imaged using fluorescent microscopy.

Images were analyzed with ImageJ to determine the circularity of cells as well as the number of live and dead cells. Fractional cell viability was calculated as

$$Fractional\ Viability = \frac{Live\ Cells}{Dead\ Cells} \times\ 100.$$

2.8. Statistical analysis

T-tests were conducted to investigate differences between groups. Results were considered significant at $P < 0.05$. All results are reported as mean ± standard deviation. Minitab 17 statistics software was used to check the significant effect of the duration of culture and the concentration of alginate for cell viability studies using ANOVA (general linear model).

3. Results and discussion

3.1. Morphology of scaffolds

The architectural properties of a scaffold are characterized in terms of its external geometry and internal structure. Figure 3 shows the indirect fabrication of scaffolds from alginate with different concentrations and the morphology of gelatin and alginate scaffolds (after refrigeration and incubation) using microscopic and SEM imaging. It shows distinct differences in the appearance of the scaffolds as well. All samples were visibly larger in area than the sacrificial gelatin, as a temporary framework.

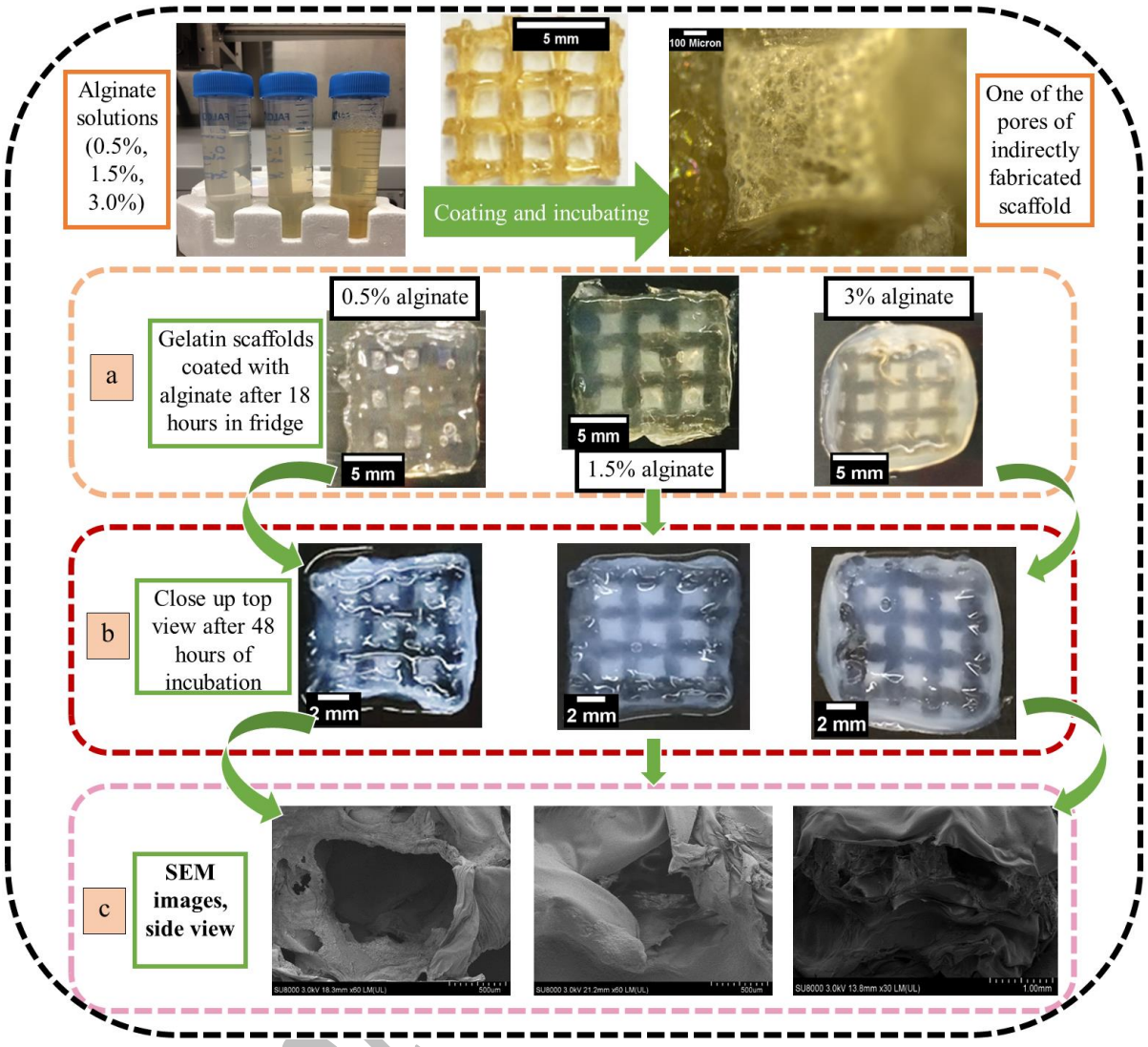

Figure 3. Indirect biofabrication of alginate scaffolds using sacrificial gelatin [from left to right: 0.5, 1.5, and 3% alginate solutions, sacrificial framework (scale bar 5 mm), and pore of indirect-fabricated scaffold after freeze-drying (scale bar 100 µm)]: a) impregnated gelatin scaffolds after 18 h refrigeration, b) removing the sacrificial material after 48 h incubation, and c) SEM images of the side view of indirectly fabricated scaffolds with 0.5%, 1.5% (scale bar 500 µm), and 3% (scale bar 1 mm) alginate concentrations after freeze-drying.

Figure 4 compares the pore size in the X and Y directions, strand diameter, and sample thickness across all sacrificial gelatin and indirectly fabricated samples after 18 h of refrigeration and 48 h of incubation. After both refrigeration and incubation, the strand diameter of all scaffolds increased compared to the original gelatin scaffold (0.763 ± 0.004 mm). A slight initial increase in pore size in all scaffolds occurred after impregnation of sacrificial frameworks with

alginate and refrigeration. However, after incubation, the pore size of all scaffolds decreased to significantly less than the original gelatin scaffold with a pore size of 1.507 ± 0.055 mm and 1.518 ± 0.061 mm in X and Y directions, respectively. Pore size, shape, and interconnectivity have a profound influence on tissue regeneration and integration. Different pore sizes are preferable for different anatomical locations to obtain functional tissue regeneration. For example, scaffolds employed in bone tissue engineering having 160-700 μm average pore size (Naghieh et al., 2016), while in vascular tissue engineering pore sizes larger than 400 μm inhibit the formation of a vascular network (Bai et al., 2010; Kruyt et al., 2003).

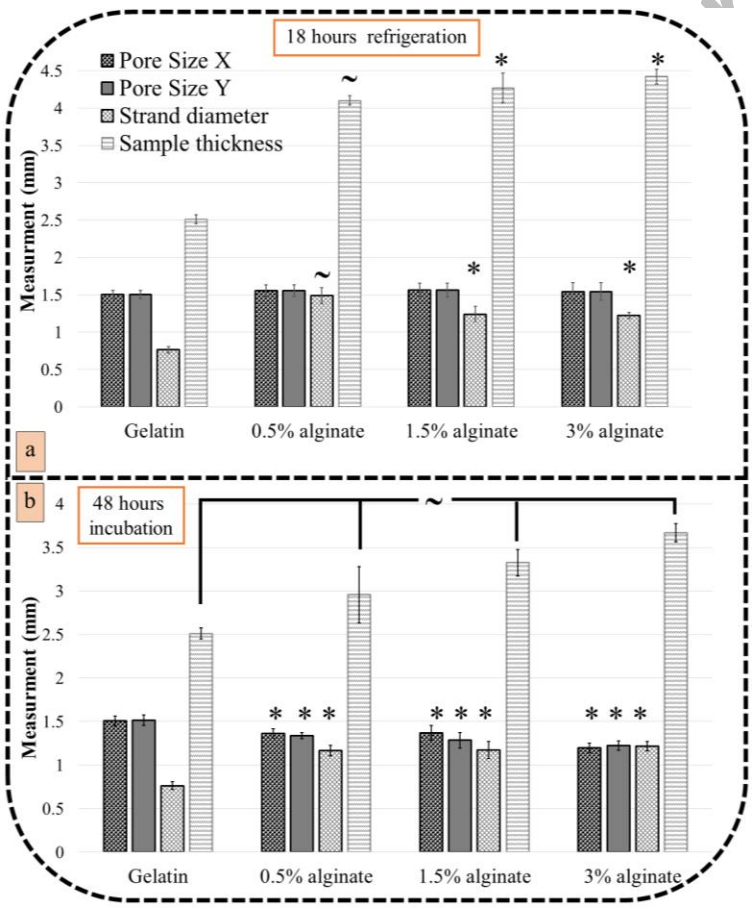

Figure 4. A comparison of pore size, strand diameter, and sample thickness from sacrificial gelatin scaffolds to samples after a) 18 h of refrigeration and b) subsequent 48 h of incubation. (*) and (~) indicate a significant difference from the original scaffold and the two other sample types, respectively ($p \leq 0.05$, $n = 9$).

3.2.Mechanical properties

Scaffolds indirectly fabricated from 0.5, 1.5, and 3.0% alginate were subjected to either ethanol disinfection, UV irradiation, or no sterilization. Compressive stress-strain tests were conducted to analyze the effect of varying %w/v concentration and method of sterilization on mechanical strength. We note here other factors beyond sterilization technique, such as crosslinking mechanism and molecular weight of the alginate, also affect mechanical properties (Freeman and Kelly, 2017; Matyash et al., 2012; Naghieh et al., 2018a). Figure 5 shows that scaffolds with a higher %w/v concentration of alginate have a higher elastic modulus. This corresponds to scaffolds with a higher solids concentration displaying greater mechanical strength. Scaffolds treated with ethanol had the highest elastic modulus, followed by unsterilized scaffolds, and then UV irradiated scaffolds. Polymers degrade when exposed to UV light (Nagai et al., 2005; Wasikiewicz et al., 2005), which is likely the cause for the decrease elastic modulus in samples sterilized with UV irradiation. Similarly, bacterial degradation might alter the structural integrity of the nonsterile hydrogel and thus affect the elastic modulus of alginate scaffolds (Arnosti et al., 1994). Based on the results above, the scaffolds treated with ethanol were determined to have the best mechanical properties (from having a higher elastic modulus point of view) and thus were subjected to swelling and degradation tests.

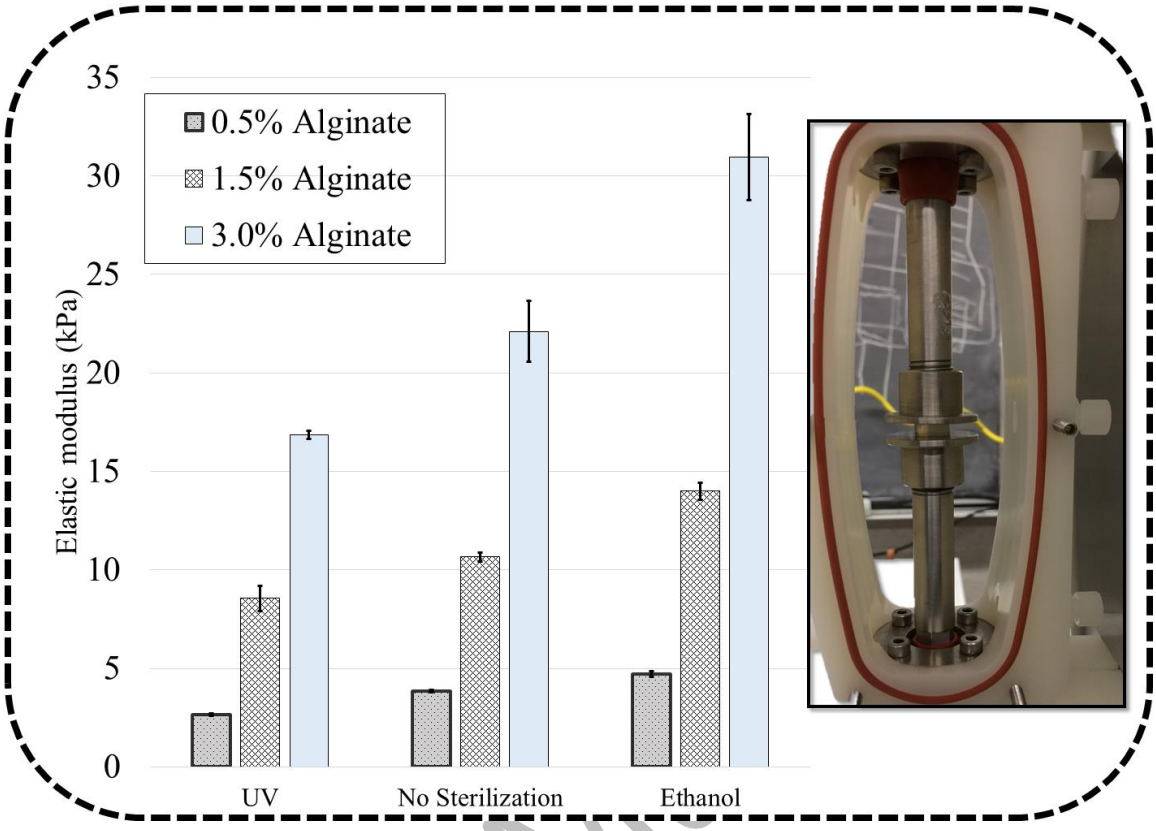

Figure 5. Elastic modulus for different scaffolds (fabricated from 0.5, 1.5, and 3% alginate) for control samples and those sterilized using UV or ethanol (results for all groups are significantly different at $p \leq 0.05$).

3.3. Swelling properties

In this study, the hydrogels were soaked in PBS. An exchange reaction occurs between the calcium (Ca^{2+}) ions in the scaffold and the sodium (Na^{+}) ions in the PBS, causing the crosslinks in the alginate formed by $CaCl_2$ to break, releasing Ca^{2+} ions into solution (Lee and Mooney, 2013). Water then enters the hydrogel and causes it to swell. Figure 6a shows the trend over 24 h for all hydrogel precursors considered (0.5, 1.5, 3%), which reflects initial swelling followed thereafter by degradation. Rapid swelling occurred in the first hour due to ion exchange, polymer chain relaxation, and water uptake. The low-concentration alginate precursor contains less mannuronic and glucuronic acid compared to the high concentration alginate precursor. In particular, carboxylate ions ($COOH^{-}$) supplied by either mannuronic or glucuronic acid participate in the crosslinking process by forming a bond with divalent ions (i.e., Ca^{2+}). The strength and density of crosslinking depends on the availability of divalent and carboxylate ions in the hydrogel. In this study, the swelling rate of the scaffolds occurred in the order 0.5% >

1.5% > 3% alginate precursor in the first hour of incubation. After the first hour, the swelling of the 1.5 and 3% alginate scaffolds continued at a slower rate due to the effect of saturation, whereas the swelling of the 0.5% alginate scaffold started decreasing at a rapid rate due to the initiation of degradation mechanisms. The swelling of 1.5 and 3% hydrogels appeared to decline after 3 and 6 h, respectively. The slower swelling rate of the 3.0% alginate compared to 1.5% alginate is attributed to its high crosslinking density and strength. The lower crosslinking density in low-concentration alginate hydrogels (0.5 and 1.5%) caused rapid degradation that reduced the swelling of these scaffolds in the PBS earlier than for the higher concentration (3%) alginate. Samples were weighed again after 1 week, but no significant change in swelling was observed. All tests were conducted in a constant volume of PBS, meaning no extra Na^+ ions were added to each well of the tissue culture plate. Once the samples reached equilibrium with surrounding Na^+ ions after 8 h of incubation, little change in the amount of swelling was identified in all samples due to insignificant polymer chain relaxation, water uptake, and degradation, in agreement with (Mendoza García et al., 2017).

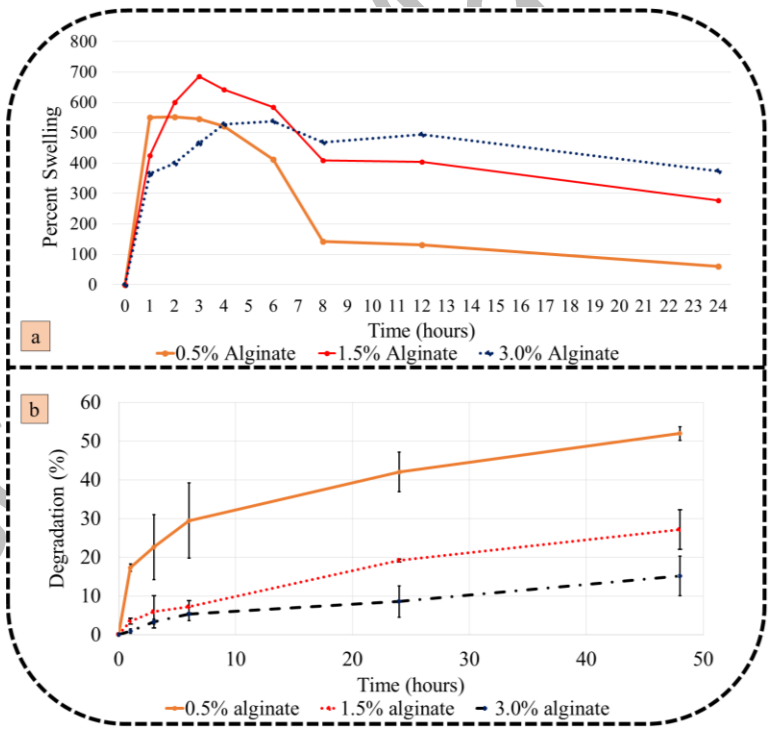

Figure 6. Percent a) swelling over 24 h and b) degradation over 48 h of the three types of alginate scaffolds created using the indirect fabrication technique.

3.4.Degradation properties

Alginate hydrogels were degraded by the release of divalent ions crosslinking the gel, in this case Ca^{2+}, into the surrounding solution by an exchange reaction with monovalent cations (Lee and Mooney, 2013), in this case the Na^{+} ions found in the PBS solution. Figure 6b shows the degradation trends of the three scaffold types (0.5, 1.5, 3% alginate precursor) over 48 h. The 0.5% alginate scaffold shows the most dramatic change, degrading 52% ± 1.74 at 48 h. In comparison, the 1.5% scaffold and the 3% scaffold both changed more gradually, degrading 27.4% ± 5.11 and 15.14% ± 5.09, respectively, after 48 h. The degradation profile of 0.5, 1.5 and 3% alginate scaffolds increased in the order 0.5%>1.5%>3%. Similar to the observations related to swelling, rapid degradation occurred in all alginate scaffolds from 0 to 3 h and then slowed due to ionic equilibrium (Na^{+}/Ca^{2+}) with the surroundings (due to the fixed volume of PBS in each culture well). Notably, both the 0.5 and 1.5% alginate samples became structurally unstable after 48 h but the 3% alginate samples maintained their structure for almost one week (results not shown).

Figure 7a shows the progression of the degradation of the alginate scaffolds. The 0.5% alginate scaffolds degraded rapidly, completely losing their physical structure after only 3 h; the 1.5% scaffolds began losing their structure after 3 h, with almost complete loss after 48 h; the 3.0% scaffolds underwent no dramatic visible change in structure over 48 h. The inner structure of the different groups was investigated using SEM imaging. Figure 7b shows the internal structure of indirect-fabricated scaffolds made from different concentrations of alginate after 24 h. Scaffolds fabricated from low-concentration alginate (0.5%) had more porous structures than those made from 3% alginate, which had a rigid structure; the porous structure might facilitate the higher rate of degradation observed in the 0.5% alginate group. After 1 hour of incubating in the PBS solution, 0.5% and 1.5% scaffolds had a smother inner structure than the 3% scaffold, which is good evidence of surface/bulk degradation as well as the dissolution of the lower concentration alginate. The 3% alginate scaffold demonstrated a rough surface even after 24 h in contrast to the other groups that showed evidence of erosion. The visual changes in Figure 7 closely follow the degradation trend in Figure 6b. The structural integrity of the 3% alginate scaffolds over 48 h suggests their possible application in tissue engineering. As the scaffolds retain well-interconnected internal channels, created using sacrificial gelatin, this type of scaffold would be useful in studying micro-fluidics and vascularization (Huang et al., 2011). In contrast, the relatively rapid degradation of the 0.5 and 1.5% alginate scaffolds could be useful in drug or

cell release studies. Low-concentration hydrogels have promise in terms of neurite outgrowth for nerve tissue engineering; being rapidly degradable, such low-concentration hydrogels could be used as a filler material inside a conduit for their possible application in nerve guidance conduits, as reported in detail elsewhere (Sarker et al., 2018).

The degradation experiments were conducted in a fixed volume of PBS and at a temperature designed to simulate the physiologic environment. Under these conditions, ion exchange takes place during the first few hours until equilibrium with the PBS is achieved. Because ion exchange is associated with degradation, observation of the degradation rate during the first few hours is critical for understanding the mechanical behavior of alginate/gelatin scaffolds in the physiologic buffer.

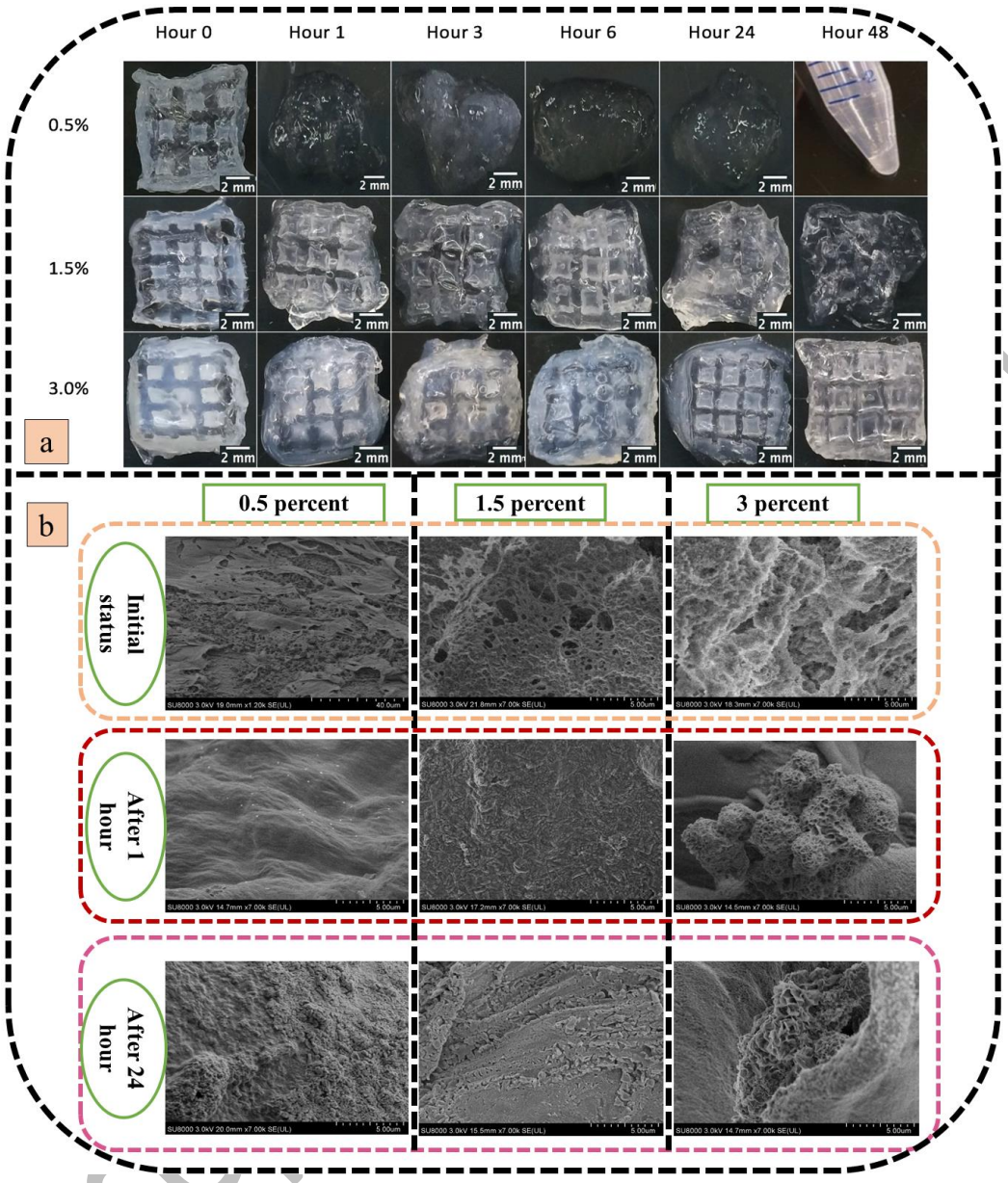

Figure 7. Progression of degradation for 1.5 and 3.0% alginate scaffolds over 48 h: a) visual observation and b) SEM images of indirect-fabricated scaffolds with 0.5, 1.5, and 3% alginate.

3.5. Cell viability and circularity assessment

3.5.1. Fluorescent imaging of bulk gels

Each bulk gel was stained with Hoechst and PI to show the number of total cells and dead cells, respectively. All hydrogels experienced a decrease in cell viability over the course of 8 d (Figure 8). The 3% and 1.5% alginate hydrogels experienced a steep drop in fractional viability from day 1 to day 8 (less than 40% and 30% for 1.5% and 3% alginate hydrogels, respectively),

while the 0.5% gel had higher cell viability at the end of day 8 (more than 50%). The cells seeded onto the 0.5% bulk gel had a higher fractional viability over 8 days than those on 1.5 and 3.0% bulk gels. This might be due to the lower concentration of this hydrogel making it a favorable substrate for cells, as reported elsewhere (Matyash et al., 2012). Increasing alginate precursor concentration results in a stiffer internal structure of the bulk gel, which interrupts diffusion mass transfer mechanism between the cells and culture media and significantly affects the metabolic mechanism of incorporated cells. In addition, strong bonds among the polymer chains in the high-concentration alginate inhibit cell migration/proliferation as well as cell to cell interactions. Therefore, high concentration alginate is not a promising biomaterial in terms of cell viability but demonstrates relatively suitable mechanical properties for tissue engineering applications. In contrast, low-concentration (0.5%) alginate demonstrates better cell viability compared to high-concentration alginate but has poorer mechanical stability. Hence, the optimum concentration of alginate precursor needs to be determined prior to fabrication to achieve both satisfactory mechanical stability and cell viability. The decreased cell viability in all alginate hydrogels with time could be improved by introducing interconnected channels through indirect printing and the creation of scaffolds with a porous structure. Such an interconnected structure would facilitate diffusive mass transfer (i.e., nutrients, oxygen gas, proteins, metabolites etc.) between the incorporated cell population and the surrounding culture medium.

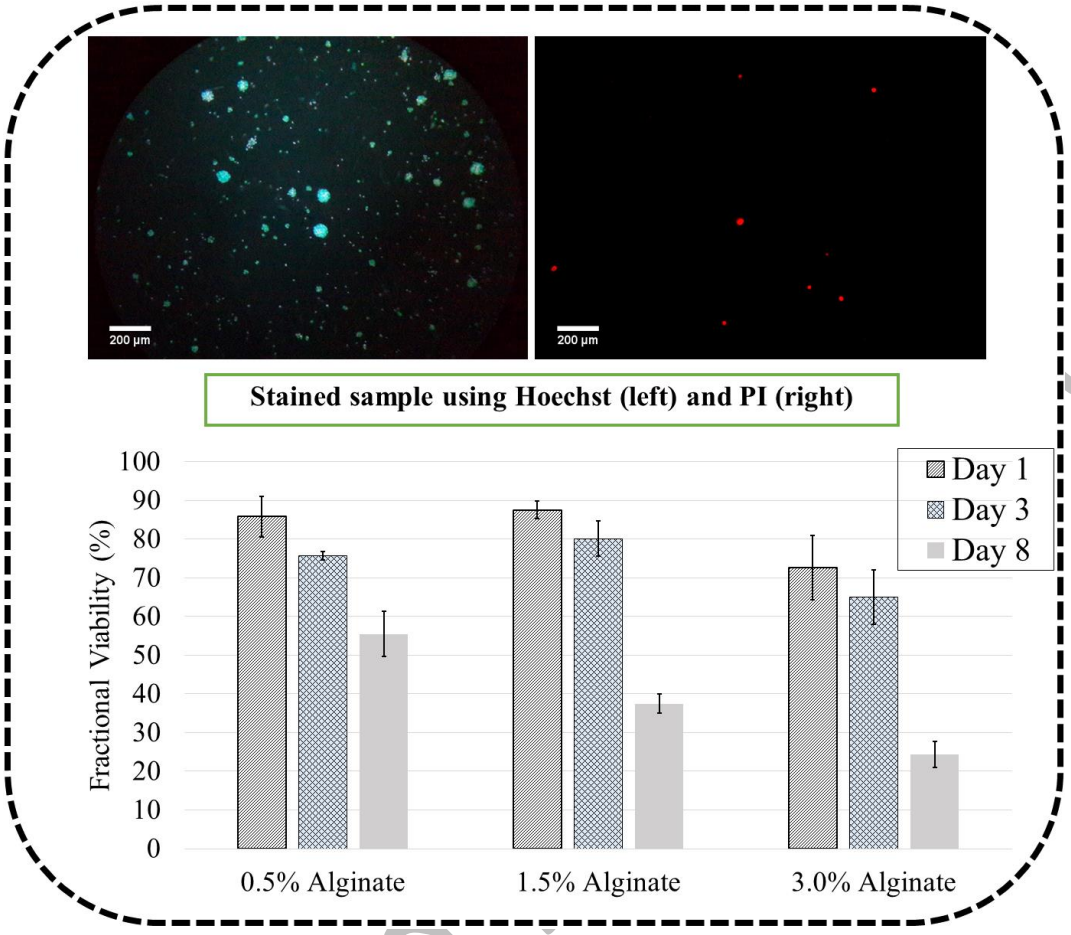

Figure 8. Fractional cell viability in 0.5, 1.5, and 3% bulk alginate gels over 8 d. Based on ANOVA (general linear model), time, concentration, and their interaction are statistically significant ($p<0.05$) (top pictures are fluorescence microscope images of the total (left) and dead (right) staining of Schwann cells using Hoechst and PI).

3.5.2. Fluorescent imaging of cell-incorporated scaffolds

Scaffolds were stained with calcein and Hoechst to show the number of live cells and total cells, respectively. Calcein staining and optical images captured from the cell-incorporated scaffolds after bioprinting are shown in Figure 9. The 0.5% alginate had poor printability (Figure 1) and so 0.5% alginate scaffolds were not considered; images in Figure 9I are for bulk gel. Optical microscopy was used to illustrate cell development, with the images showing pores were open and cells were well distributed (partially elongated cells with high cell density; Figure 9II and III). Alginate scaffolds fabricated with 1.5 or 3.0% hydrogel precursor showed better cell viability compared to 0.5% alginate gel on day 3 and 8 due to the interconnected bioplotted structures (Figure 10). However, alginate scaffolds printed with 3% alginate precursor

demonstrated poorer cell viability than the 1.5% alginate scaffold, indicating the effect of shear stress-induced cell damage during the bioplotting process. Live cells within the 0.5% bulk alginate gel showed a decreasing trend over the 8 d of *in vitro* culture; this is attributed to rapid degradation and the non-porous structure. Incorporated Schwann cells in 1.5 and 3.0% alginate scaffolds had a higher cell viability at day 3 than day 1 or 8 that might be due to the high proliferation rate; the observed decrease in cell viability thereafter is likely due to the effect of tissue remodeling. Compared to 3% alginate scaffolds, 1.5% alginate scaffolds maintained better cell viability over the 1 to 8 day culture period, suggesting the efficacy of less stiff polymer in the 3D cell incorporation approach. These results suggest the potential for scaffolds bioplotted with sequential layers of soft and stiff hydrogel strands, which would simultaneously address both biological and mechanical performance for specific tissue engineering applications.

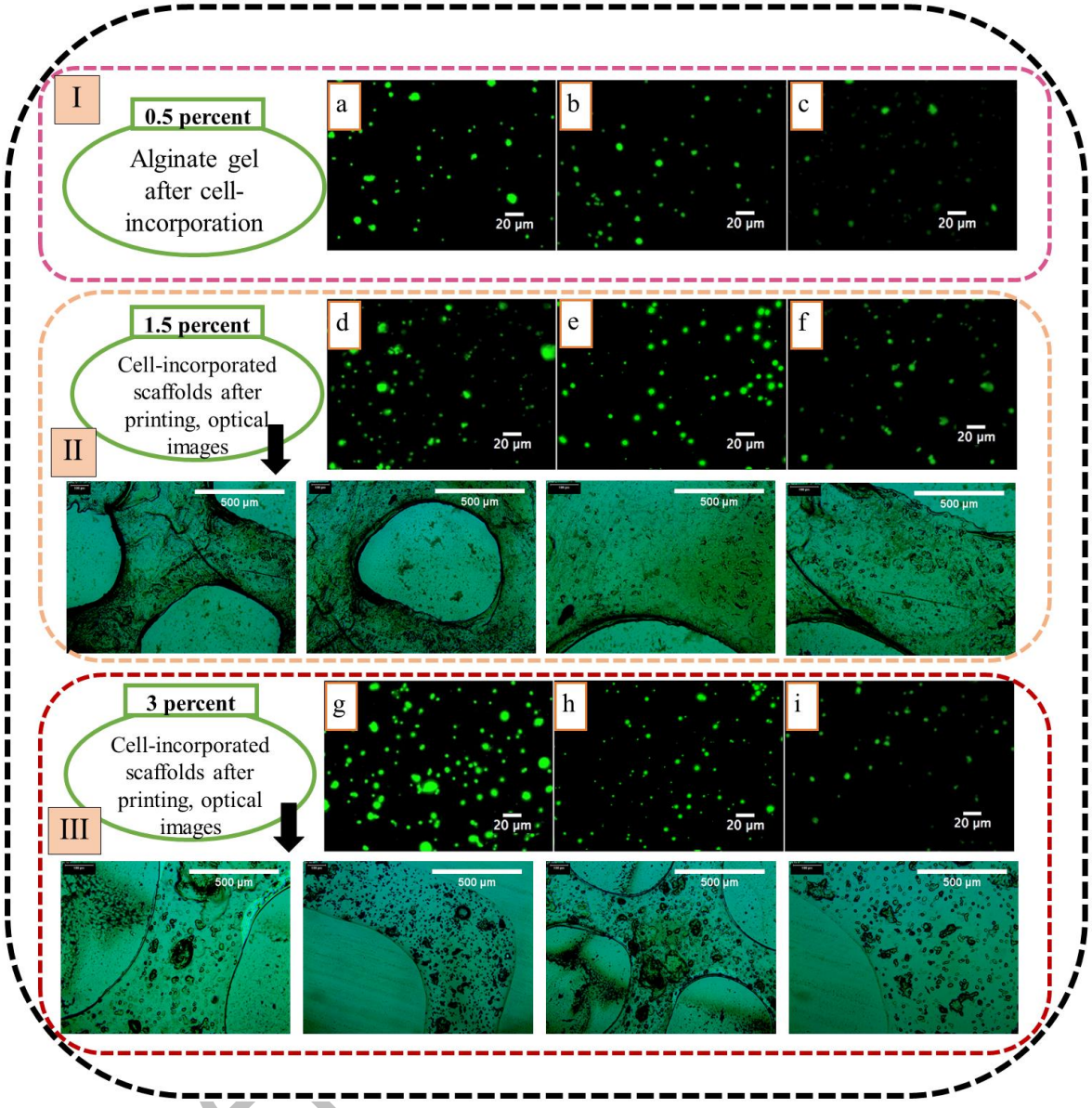

Figure 9. Fluorescence microscope images of live staining of Schwann cells (scale bar 20 µm) showing live cells: I) 0.5% alginate bulk gel: a) day 1, b) day 4, c) day 8; II) 1.5% alginate scaffold: d) day 1, e) day 4, f) day 8; III) 3% alginate scaffold: g) day 1, h) day 4, i) day 8 (optical images in II and III were captured after fabrication of the cell-incorporated scaffolds; all scale bars are 500 µm).

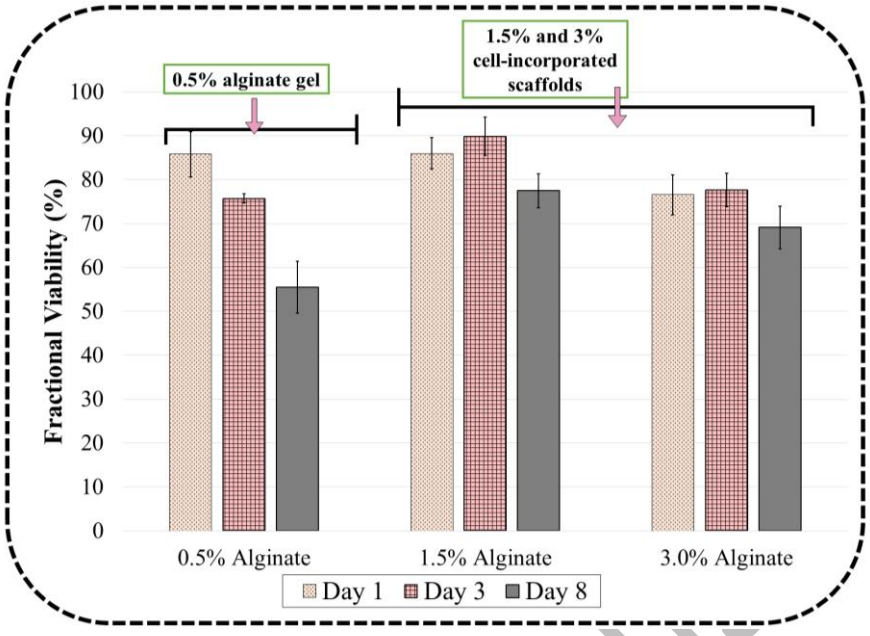

Figure 10. Fractional cell viability in each cell-incorporated scaffold after 8 d. Error bars are standard deviation. Based on ANOVA (general linear model), time, concentration, and their interaction are statistically significant ($p<0.05$).

3.6. Cell morphology in bulk gels and cell-incorporated/post-seeded scaffolds

Calcein assay was used to stain the cytoplasm of Schwann cells to assess the morphology of cells over time (DeCoster et al., 2010). The circularity of cells in the three types of alginate structures was analyzed using ImageJ. Circularity is measured on a 0.0-1.0 scale, with 1.0 being a perfect circle. Low circularity values are associated with a more stretched, attached, or differentiated state of incorporated cells. The circularity of cells in the 0.5, 1.5, and 3.0% alginate bulk gels was 0.423 ± 0.118, 0.768 ± 0.034, and 0.799 ± 0.064, respectively, after 8 d (Figure 11a). The lower circularity of cells in the 0.5% alginate gel at day 8 compared to other groups occurred concurrently with rapid degradation during the culture period due to significant polymer chain relaxation, swelling, and medium uptake within the bulk gel. Absorption of culture medium facilitated the availability of various protein molecules within the matrix that helped Schwann cells in the 0.5% alginate hydrogel express multipolar morphology. The higher values for cell circularity for the other bulk gels (3 and 1.5%; Figure 11a) suggest the lower concentration of alginate is more favorable for 3D Schwann cell cultures over time.

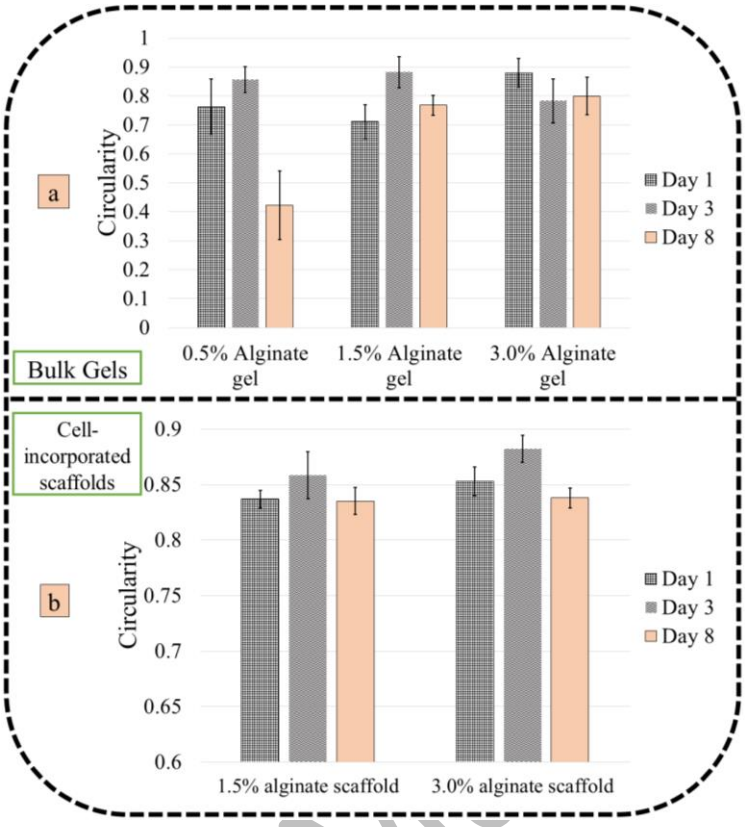

Figure 11. Cell circularity on bulk gels and cell-incorporated scaffolds over 8 d.

In the 1.5 and 3% alginate scaffolds fabricated using direct bioplotting (Figure 11b), incorporated cells were more circular than in the 0.5% alginate bulk gel (Figure 11a). The high circularity is attributed to confined cells that are unable to migrate and interact with each other inside the alginate strands of the bioplotted scaffolds. Furthermore, the trend in Figure 11b indicates that the circularity of cells in the 1.5 and 3% alginate scaffolds are close to 0.9 at day 3. This might be due to a large number of cells, resulting from cell proliferation, becoming trapped in a confined space, where they tend to remain in a more circular shape. This could also explain the spike in circularity on day 3 for both the 1.5 and 3.0% alginate scaffolds (cell retraction due to proliferation). On a 2D tissue culture plate, Schwann cells usually demonstrate multipolar morphology, extending multiple processes that are indicative of attachment, differentiation, and migrated states. In the *in vivo* state, the morphology might differ from cell to cell as per the location and function of the tissue or organ. In some applications, spherical morphology of cells (such as chondrocytes and pancreatic islet cells) incorporated into alginate hydrogel can form functional tissues (Calafiore, 2003; Chia et al., 2004); however, the elongated morphology of

Schwann cells is expected in a 3D culture to facilitate the formation Bands of Büngner necessary for the regeneration of damaged peripheral nerves.

Figure 12a shows an increase in circularity over 8 days for post-seeded scaffolds. Figure 12b demonstrates an increase in cells and cell clumping, and therefore the increased circularity again might be due to the retraction of cells to make space for proliferating cells. Figure 12b also shows the Schwann cells attached to the surface of the indirect-fabricated scaffolds. Schwann cells continued to proliferate on the surface of the 0.5% alginate scaffold to day 8 (Figure 12b), but this was less evident for the other alginate scaffolds (1.5 and 3%). This is consistent with reports demonstrating the limitations of cell migration, growth, and differentiation using high-density hydrogels (Zehnder et al., 2015). As shown in Figure 7b, pores are evident in the inner structure of the 0.5% indirect-fabricated scaffolds and could facilitate the observed cell growth. Furthermore, not only were more cells observed on the surface of 0.5% alginate scaffold, for all sample groups, the seeded cells showed more spherical morphology over time in particular spots on the alginate surface, indicative of cell proliferation. It is well-established that polysaccharide molecules lacking peptides in their structure do not facilitate cell attachment on the surface. However, absorption of gelatin molecules released from the indirectly-fabricated framework on the surface of alginate strands might enhance the surface properties of alginate scaffolds fabricated by the proposed indirect approach. Moreover, some amount of gelatin might get absorbed in the alginate hydrogel during the removal process, and thereafter have a positive effect on the cellular behavior (You et al., 2016).

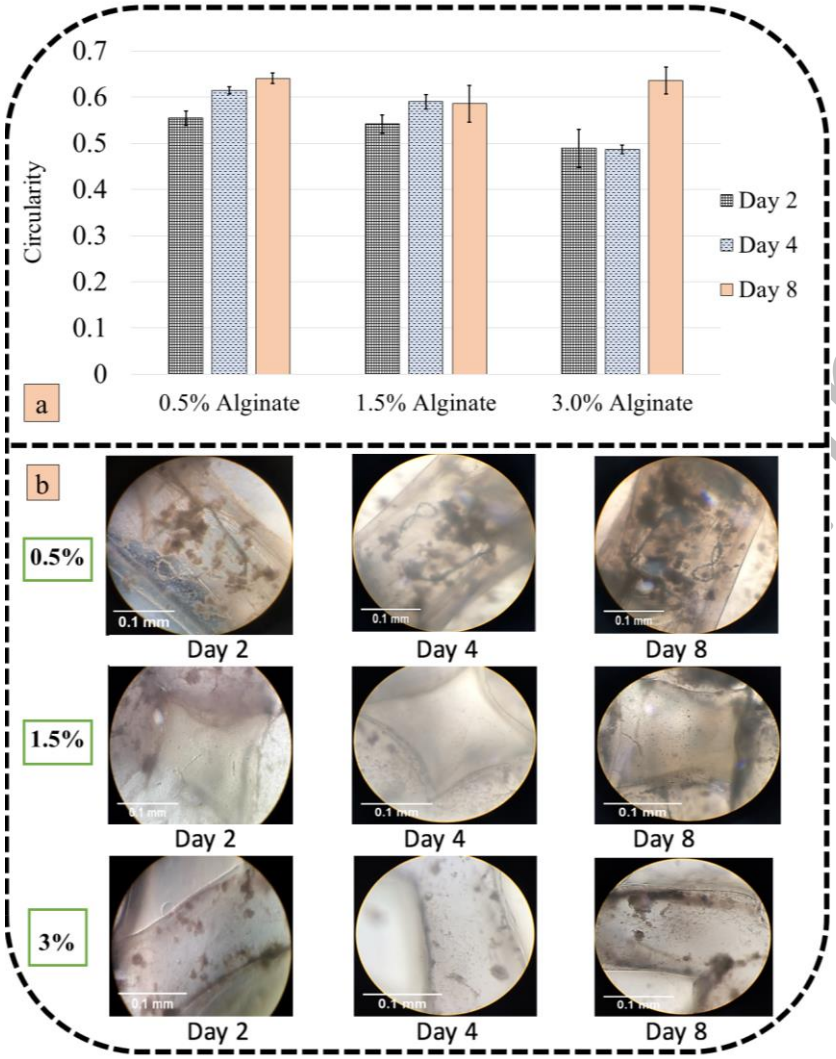

Figure 12. Cell circularity of Schwann cells in post-seeded scaffolds over 8 d: a) cell viability for different groups of indirect-fabricated scaffolds and b) optical images from samples from different days indicating the morphology of cells (100× magnification).

4. Conclusions

Hydrogels are widely used in the bioprinting of scaffolds for tissue engineering applications. Low-concentration hydrogels create a favorable environment for many cell functions but are limited from the fabrication point of view due to poor printability. Here, we illustrated the feasibility of fabricating scaffolds from low-concentration alginate using an indirect-bioprinting process by means of a sacrificial gelatin framework. Scaffolds were fabricated with varying concentrations of alginate and then sterilized using either UV or ethanol. Next, the scaffolds were characterized biologically using Schwann cells for potential nerve tissue

engineering applications. Our results indicate that scaffolds can be fabricated by the indirect-bioprinting process at precursor alginate concentrations of 0.5-3%. Scaffolds created from 0.5, 1.5, and 3% alginate and sterilized with ethanol have a higher elastic modulus than those treated with UV. Scaffolds made from 0.5 and 1.5% alginate experienced significant changes in swelling, while those fabricated from 3.0% alginate demonstrated much more gradual changes. In addition, 0.5% alginate scaffolds experienced dramatic degradation compared to those fabricated from 1.5 or 3.0% alginate. The low-concentration alginate scaffolds provided a more favorable environment for Schwann cells. Taken together, our results show the indirect-bioprinting process successfully addresses the poor printability of low-concentration alginate for scaffold fabrication. The results further show that both the mechanical and biological properties of fabricated scaffolds are affected by the concentration of alginate as well as the sterilization technique utilized. These results provide an effective means of regulating scaffold properties during the indirect-bioprinting process. Furthermore, the results indicate the possibility of extending the proposed indirect-bioprinting process to other types of low-concentration hydrogels to address the tradeoffs between printability and properties favorable for cell functioning.

Acknowledgments

The authors acknowledge Dr. David Schreyer (Department of Anatomy and Cell Biology of the University of Saskatchewan) and Dr. Adam McInnes (Division of Biomedical Engineering of the University of Saskatchewan) for contributing to valuable discussions. Cell culture and examinations were conducted at Saskatoon City Hospital with the help of Dr. Schreyer. Financial support from the Natural Sciences and Engineering Research Council of Canada (NSERC, grant number RGPIN-2014-05648) is also acknowledged.

References:

Arnosti, C., Repeta, D.J., Blough, N. V, 1994. Rapid bacterial degradation of polysaccharides in anoxic marine systems. Geochim. Cosmochim. Acta 58, 2639–2652.

Augst, A.D., Kong, H.J., Mooney, D.J., 2006. Alginate hydrogels as biomaterials. Macromol. Biosci. 6, 623–633.

Bai, F., Wang, Z., Lu, J., Liu, J., Chen, G., Lv, R., Wang, J., Lin, K., Zhang, J., Huang, X., 2010. The correlation between the internal structure and vascularization of controllable porous bioceramic materials in vivo: a quantitative study. Tissue Eng. Part A 16, 3791–3803.

Bertassoni, L.E., Cardoso, J.C., Manoharan, V., Cristino, A.L., Bhise, N.S., Araujo, W.A.,

Zorlutuna, P., Vrana, N.E., Ghaemmaghami, A.M., Dokmeci, M.R., 2014. Direct-write Bioprinting of Cell-laden Methacrylated Gelatin Hydrogels. Biofabrication 6, 1–19. doi:10.1088/1758-5082/6/2/024105.Direct-write

Calafiore, R., 2003. Alginate microcapsules for pancreatic islet cell graft immunoprotection: struggle and progress towards the final cure for type 1 diabetes mellitus.

Cao, N., Chen, X.B., Schreyer, D.J., 2012. Influence of Calcium Ions on Cell Survival and Proliferation in the Context of an Alginate Hydrogel. ISRN Chem. Eng. 2012, 1–9. doi:10.5402/2012/516461

Chia, S.H., Schumacher, B.L., Klein, T.J., Thonar, E.J., Masuda, K., Sah, R.L., Watson, D., 2004. Tissue-engineered human nasal septal cartilage using the alginate-recovered-chondrocyte method. Laryngoscope 114, 38–45.

DeCoster, M.A., Maddi, S., Dutta, V., McNamara, J., 2010. Microscopy and image analysis of individual and group cell shape changes during apoptosis. Microsc. Sci. Technol. Appl. Educ.

England, S., Rajaram, A., Schreyer, D.J., Chen, X., 2017. Bioprinted fibrin-factor XIII-hyaluronate hydrogel scaffolds with encapsulated Schwann cells and their in vitro characterization for use in nerve regeneration. Bioprinting 5, 1–9. doi:10.1016/j.bprint.2016.12.001

Freeman, F.E., Kelly, D.J., 2017. Tuning Alginate Bioink Stiffness and Composition for Controlled Growth Factor Delivery and to Spatially Direct MSC Fate within Bioprinted Tissues. Sci. Rep. 1–12. doi:10.1038/s41598-017-17286-1

He, Y., Yang, F., Zhao, H., Gao, Q., Xia, B., Fu, J., 2016. Research on the printability of hydrogels in 3D bioprinting. Sci. Rep. 6, 29977. doi:10.1038/srep29977

Houben, A., Van Hoorick, J., Van Erps, J., Thienpont, H., Van Vlierberghe, S., Dubruel, P., 2017. Indirect Rapid Prototyping: Opening Up Unprecedented Opportunities in Scaffold Design and Applications. Ann. Biomed. Eng. doi:10.1007/s10439-016-1610-x

Huang, G.Y., Zhou, L.H., Zhang, Q.C., Chen, Y.M., Sun, W., Xu, F., Lu, T.J., 2011. Microfluidic hydrogels for tissue engineering. Biofabrication 3, 12001.

Kruyt, M.C., de Bruijn, J.D., Wilson, C.E., Oner, F.C., van Blitterswijk, C.A., Verbout, A.J., Dhert, W.J.A., 2003. Viable Osteogenic Cells Are Obligatory for Tissue-Engineered Ectopic Bone Formation in Goats. Tissue Eng. 9, 327–336. doi:10.1089/107632703764664792

Lee, K.Y., Mooney, D.J., 2013. Alginate : properties and biomedical applications. Prog. Polym. Sci. 37, 106–126. doi:10.1016/j.progpolymsci.2011.06.003.Alginate

LeRoux, M. a, Guilak, F., Setton, L. a, 1999. Compressive and shear properties of alginate gel: Effects\nof sodium ions and alginate concentration. J. Biomed. Mater. Res. 47, 46–53. doi:10.1002/(SICI)1097-4636(199910)47

Li, M., Tian, X., Zhu, N., Schreyer, D.J., Chen, X., 2009. Modeling process-induced cell damage in the biodispensing process. Tissue Eng. Part C Methods 16, 533–542.

Matyash, M., Despang, F., Mandal, R., Fiore, D., Gelinsky, M., Ikonomidou, C., 2012. Novel Soft Alginate Hydrogel Strongly Supports Neurite Growth and Protects Neurons Against Oxidative Stress. Tissue Eng. Part A 18, 55–66. doi:10.1089/ten.tea.2011.0097

Mendoza García, M., Izadifar, M., Chen, X., 2017. Evaluation of PBS Treatment and PEI Coating Effects on Surface Morphology and Cellular Response of 3D-Printed Alginate Scaffolds. J. Funct. Biomater. 8, 48. doi:10.3390/jfb8040048

Nagai, N., Matsunobe, T., Imai, T., 2005. Infrared analysis of depth profiles in UV-

photochemical degradation of polymers. Polym. Degrad. Stab. 88, 224–233. doi:10.1016/j.polymdegradstab.2004.11.001

Naghieh, S., Chen, X.B., 2019. Scaffold Design, in: Extrusion Bioprinting of Scaffolds for Tissue Engineering Applications. Springer International Publishing Switzerland. doi:10.1007/978-3-030-03460-3

Naghieh, S., Karamooz-Ravari, M.R., Sarker, M., Karki, E., Chen, X., 2018a. Influence of crosslinking on the mechanical behavior of 3D printed alginate scaffolds: Experimental and numerical approaches. J. Mech. Behav. Biomed. Mater. 80, 111–118. doi:10.1016/j.jmbbm.2018.01.034

Naghieh, S., Karamooz Ravari, M.R.R., Badrossamay, M., Foroozmehr, E., Kadkhodaei, M., 2016. Numerical investigation of the mechanical properties of the additive manufactured bone scaffolds fabricated by FDM: the effect of layer penetration and post-heating. J. Mech. Behav. Biomed. Mater. 59, 241–250. doi:10.1016/j.jmbbm.2016.01.031

Naghieh, S., Sarker, M., Izadifar, M., Chen, X., 2018b. Dispensing-based bioprinting of mechanically-functional hybrid scaffolds with vessel-like channels for tissue engineering applications – a brief review. J. Mech. Behav. Biomed. Mater. 78, 298–314. doi:10.1016/j.jmbbm.2017.11.037

Ning, L., Sun, H., Lelong, T., Guilloteau, R., Zhu, N., Schreyer, D.J., Chen, D.X., 2018. 3D bioprinting of scaffolds with living Schwann cells for potential nerve tissue engineering applications. Biofabrication.

Ning, L., Xu, Y., Chen, X., Schreyer, D.J., 2016. Influence of mechanical properties of alginate-based substrates on the performance of Schwann cells in culture. J. Biomater. Sci. Polym. Ed. 27, 898–915.

Potjewyd, G., Moxon, S., Wang, T., Domingos, M., Hooper, N.M., 2018. Tissue Engineering 3D Neurovascular Units: A Biomaterials and Bioprinting Perspective. Trends Biotechnol.

Rajaram, A., Schreyer, D.J., Chen, D.X.B., 2015. Use of the polycation polyethyleneimine to improve the physical properties of alginate–hyaluronic acid hydrogel during fabrication of tissue repair scaffolds. J. Biomater. Sci. Polym. Ed. 26, 433–445.

Sarker, M. d., Naghieh, S., Mcinnes, A.D., Schreyer, D.J., Chen, X., 2018. Strategic design and fabrication of nerve guidance conduits for peripheral nerve regeneration. Biotechnol. J. 1700635. doi:10.1002/biot.201700635

Skardal, A., Devarasetty, M., Kang, H.-W., Mead, I., Bishop, C., Shupe, T., Lee, S.J., Jackson, J., Yoo, J., Soker, S., 2015. A hydrogel bioink toolkit for mimicking native tissue biochemical and mechanical properties in bioprinted tissue constructs. Acta Biomater. 25, 24–34.

Stoppel, W., White, J.C., Horava, S.D., Roberts, S.C., Stoppel, W.L., White, J.C., Horava, S.D., Henry, A.C., Roberts, S.C., Bhatia, S.R., 2014. Terminal sterilization of alginate hydrogels : Efficacy and impact on mechanical properties on mechanical properties. doi:10.1002/jbm.b.33070

Sun, J., Tan, H., 2013. Alginate-Based Biomaterials for Regenerative Medicine Applications 1285–1309. doi:10.3390/ma6041285

Tamjid, E., Simchi, A., 2015. Fabrication of a highly ordered hierarchically designed porous nanocomposite via indirect 3D printing: Mechanical properties and in vitro cell responses. Mater. Des. 88, 924–931.

Tan, J.Y., Chua, C.K., Leong, K.F., 2010. Indirect fabrication of gelatin scaffolds using rapid prototyping technology. Virtual Phys. Prototyp. 5, 45–53. doi:10.1080/17452751003759144

Tan, Y.J., Tan, X., Yeong, W.Y., Tor, S.B., 2016. Hybrid microscaffold-based 3D bioprinting of multi-cellular constructs with high compressive strength: A new biofabrication strategy. Sci. Rep. 6, 39140.

Vijayavenkataraman, S., Yan, W.-C., Lu, W.F., Wang, C.-H., Fuh, J.Y.H., 2018. 3D bioprinting of tissues and organs for regenerative medicine. Adv. Drug Deliv. Rev.

Wasikiewicz, J.M., Yoshii, F., Nagasawa, N., Wach, R.A., Mitomo, H., 2005. Degradation of chitosan and sodium alginate by gamma radiation, sonochemical and ultraviolet methods. Radiat. Phys. Chem. 73, 287–295. doi:10.1016/j.radphyschem.2004.09.021

Yeong, W., Chua, C., Leong, K., Chandrasekaran, M., Lee, M., 2006. Indirect fabrication of collagen scaffold based on inkjet printing technique. Rapid Prototyp. J. 12, 229–237. doi:10.1108/13552540610682741

You, F., Wu, X., Chen, X., 2016. 3D Printing of Porous Alginate/gelatin Hydrogel Scaffolds and Their Mechanical Property Characterization. J. Int. J. Polym. Mater. Polym. Biomater. 66, 299–306. doi:10.1080/00914037.2016.1201830

Zehnder, T., Sarker, B., Boccaccini, A.R., Detsch, R., 2015. Evaluation of an alginate-gelatine crosslinked hydrogel for bioplotting. Biofabrication 7, 025001. doi:10.1088/1758-5090/7/2/025001

Figure captions:

Figure 1. 3D bioplotting of alginate hydrogels: a) cultivated Schwann cells mixed with alginate hydrogel and then bioplotted, b) cell-incorporated alginate scaffold and staining result showing one strand, and c) poor printability of 0.5% alginate printed with a 100-µm needle and staining result of cell-incorporated gel.

Figure 2. Indirect biofabrication: a) 3D bioplotter used for the fabrication of gelatin scaffolds, b) gelatin scaffold and bulk gel samples, and c) gelatin scaffold used for indirect biofabrication and a close-up view of this sacrificial framework.

Figure 3. Indirect biofabrication of alginate scaffolds using sacrificial gelatin [from left to right: 0.5, 1.5, and 3% alginate solutions, sacrificial framework (scale bar 5 mm), and pore of indirect-fabricated scaffold after freeze-drying (scale bar 100 µm)]: a) impregnated gelatin scaffolds after 18 h refrigeration, b) removing the sacrificial material after 48 h incubation, and c) SEM images of the side view of indirectly fabricated scaffolds with 0.5%, 1.5% (scale bar 500 µm), and 3% (scale bar 1 mm) alginate concentrations after freeze-drying.

Figure 4. A comparison of pore size, strand diameter, and sample thickness from sacrificial gelatin scaffolds to samples after a) 18 h of refrigeration and b) subsequent 48 h of incubation. (*) and (~) indicate a significant difference from the original scaffold and the two other sample types, respectively ($p \leq 0.05$, $n = 9$).

Figure 5. Elastic modulus for different scaffolds (fabricated from 0.5, 1.5, and 3% alginate) for

control samples and those sterilized using UV or ethanol (results for all groups are significantly different at $p \leq 0.05$).

Figure 6. Percent a) swelling over 24 h and b) degradation over 48 h of the three types of alginate scaffolds created using the indirect fabrication technique.

Figure 7. Progression of degradation for 1.5 and 3.0% alginate scaffolds over 48 h: a) visual observation and b) SEM images of indirect-fabricated scaffolds with 0.5, 1.5, and 3% alginate.

Figure 8. Fractional cell viability in 0.5, 1.5, and 3% bulk alginate gels over 8 d. Based on ANOVA (general linear model), time, concentration, and their interaction are statistically significant ($p<0.05$) (top pictures are fluorescence microscope images of the total (left) and dead (right) staining of Schwann cells using Hoechst and PI).

Figure 9. Fluorescence microscope images of live staining of Schwann cells (scale bar 20 μm) showing live cells: I) 0.5% alginate bulk gel: a) day 1, b) day 4, c) day 8; II) 1.5% alginate scaffold: d) day 1, e) day 4, f) day 8; III) 3% alginate scaffold: g) day 1, h) day 4, i) day 8 (optical images in II and III were captured after fabrication of the cell-incorporated scaffolds; all scale bars are 500 μm).

Figure 10. Fractional cell viability in each cell-incorporated scaffold after 8 d. Error bars are standard deviation. Based on ANOVA (general linear model), time, concentration, and their interaction are statistically significant ($p<0.05$).

Figure 11. Cell circularity on bulk gels and cell-incorporated scaffolds over 8 d.

Figure 12. Cell circularity of Schwann cells in post-seeded scaffolds over 8 d: a) cell viability for different groups of indirect-fabricated scaffolds and b) optical images from samples from different days indicating the morphology of cells (100× magnification).